Chemical Science

ROYAL SOCIETY OF CHEMISTRY

EDGE ARTICLE

View Article Online
View Journal | View Issue

Cite this: *Chem. Sci.*, 2024, **15**, 4054

All publication charges for this article have been paid for by the Royal Society of Chemistry

Pyrazinacene conjugated polymers: a breakthrough in synthesis and unraveling the conjugation continuum†

Fatima Hameed,‡[ab] Arindam Maity,‡[ab] Victor S. Francis[ab] and Nagarjuna Gavvalapalli *[ab]

Pyrazinacenes are next generation N-heteroacenes and represent a novel class of stable n-type materials capable of accepting more than one electron and displaying intriguing features, including prototropism, halochromism, and redox chromism. Astonishingly, despite a century since their discovery, there have been no reports on the conjugated polymers of pyrazinacenes due to unknown substrate scope and lack of pyrazinacene monomers that are conducive to condensation polymerization. Breaking through these challenges, in this work, we report the synthesis of previously undiscovered and highly coveted conjugated polymers of pyrazinacenes. In order to understand the intricacies of conjugation extension within the acene and along the polymer backbone, a series of electronically diverse four pyrazinacene conjugated polymers were synthesized. Polymers synthesis required optimizing a few synthetic steps along the 12-step synthetic pathway. The generated pyrazinacene monomers are not amenable to the popular condensation polymerizations involving Pd or Cu catalysts. Gratifyingly, Pd and Cu free dehydrohalogenation polymerization of the monomer with $HgCl_2$ resulted in high molecular weight organometallic conjugated pyrazinacene polymers within a few minutes at room temperature. The dual role played by the Hg(II) during the polymerization, combined with the self-coupling of the RHgCl (intermediate), is at the core of successful polymerization. Notably, the self-coupling of intermediates challenges the strict stoichiometric balance typically required for step-growth polymerization and offers a novel synthetic strategy to generate high molecular weight conjugated polymers even with imbalanced monomer stoichiometries. A combination of electrochemical studies and DFT-B3LYP simulations indicated that the presence of the reduced pyrazine ring promotes interacene π-conjugation through the metal center, in contrast to completely oxidized tetrazaazaanthracene. The extension of conjugation results in *ca.* 2 eV lower reduction potential for polymers compared to the monomer, placing the LUMO energy levels of these polymers on par with some of the best-known n-type polymers. Also, the presence of NH protons in the pyrazinacene polymers show ionochromism and red-shift UV-vis absorption maximum by *ca.* 100 nm. This work not only shows a way to realize highly desirable and elusive pyrazinacene conjugated polymers but also paves the way for a library of n-type conjugated polymers that can undergo multi-electron reduction.

Received 6th December 2023
Accepted 29th January 2024

DOI: 10.1039/d3sc06552a

rsc.li/chemical-science

1. Introduction

The delocalization of π-electrons of the repeat unit along the conjugated polymer backbone lowers the band gap and leads to a red-shift in the absorption spectra of the polymer and enables intrachain charge transport relative to individual monomeric units. Furthermore, the polymer's chain length and architecture offer several indispensable properties, including processability, mechanical flexibility, self-healing, and stretchability. These properties not only simplify device fabrication but also enhance device performance and lifetime.[1–13] Thus, polymerization typically transforms an ineffectual monomeric unit into a solution-processable organic semiconductor material with tunable optoelectronic and mechanical properties. Polymerization has been shown to have a positive impact not only on small aromatic molecules but also on fused acenes. The development of polymeric acenes has resulted in significant enhancements in properties for electronic and optoelectronic applications when compared to the properties of individual acene units.[14,15] Polymeric acenes also overcome challenges associated with

[a]*Department of Chemistry, Georgetown University, USA. E-mail: ng554@georgetown.edu*

[b]*Institute for Soft Matter Synthesis and Metrology, Georgetown University, Washington, D.C., 20057, USA*

† Electronic supplementary information (ESI) available. See DOI: https://doi.org/10.1039/d3sc06552a

‡ These authors contributed equally.

pure acenes, such as solubility and stability. For example, Bao *et al.* showed conjugated polymers of pentacene are air-stable and solution-processable, unlike pentacene small molecules.[16,17] This breakthrough has inspired the emergence of various functionalized acene oligomers and polymers that are both soluble and stable.[5,8,18–23] In terms of electronic structure, recent studies have demonstrated that acene-based polymers exhibit non-linear band gap alterations as the size of the carbocyclic acene unit changes, and a zero-band gap conjugated polymer of pentacene was synthesized.[24] Thus, the polymerization of acenes generates functional polymers with several indispensable features that are not accessible in small molecules.

While carbocyclic acenes primarily demonstrate p-type characteristics, significant efforts have been channeled into the creation of n-type acenes by replacing C–H groups with electronegative nitrogen atoms. Nitrogen atoms are intricately integrated into the aromatic framework of N-heteroacenes. The strategic placement of nitrogen atoms within the acenes serves to stabilize the frontier molecular orbitals (FMO), increase the electron affinity, and invert the electronic behavior of acenes, *i.e.*, instead of hole transport, azaacenes show electron transport behavior. Pyrazinacenes represent the next generation of N-heteroacenes having high nitrogen content and are composed of linearly fused pyrazine units, including dihydropyrazine groups. The linearly fused pyrazine rings enable pyrazinacenes to undergo multi-electron reduction and contribute to the stabilization of the reduced states. Additionally, the presence of multiple nitrogen atoms in the acene leads to the tautomerization of NH protons in these compounds. The NH protons on the dihydropyrazines can be deprotonated in the presence of anions, resulting in changes in the band gap, energy levels, and optoelectronic properties. Electron-deficient pyrazinacenes interact with anions through hydrogen bonding and anion–π interactions, which are fundamental in many biological processes and hence can be used as markers, sensors, and dyes in medicinal applications.[25–35] The presence of electron-deficient pyrazine rings also makes pyrazinacenes less susceptible to degradation through oxidation or dimerization, making them more stable than their carbocyclic acene counterparts. Consequently, pyrazinacenes represent a novel class of stable n-type materials capable of accepting more than one electron and displaying intriguing features, including prototropism, halochromism, and redox chromism.[36–43] Considering the array of applications in various fields, the conjugated polymers of pyrazinacenes will be of immense interest and useful in multiple areas including organic electronics, energy conversion and storage, electrochemical transistors, catalysis, and sensors. Surprisingly, to date, there have been no reports on the conjugated polymers of pyrazinacenes.

The key reasons for no reports on the synthesis of conjugated polymers of pyrazinacenes, even after a century since their first discovery, are twofold. First, the lack of pyrazinacene monomers that are conducive to condensation polymerization, resulting in soluble conjugated polymers, has been a significant obstacle. Second, the intricacies of pyrazinacene substrates' scope and the stability of linearly fused pyrazine rings when subjected to condensation polymerizations remain unknown. Breaking through these challenges, in this work, we report the synthesis of previously undiscovered and highly coveted conjugated polymers of pyrazinacenes (Fig. 1). As mentioned earlier, the polymerization of pyrazinacene chromophores is expected to enhance the performance of the materials towards various applications due to the extension of π-conjugation along the chain and molecular wire effect. As the pyrazinacene monomer is polymerized through the terminal fused ring of the acene, the intricacies of conjugation extension within the acene and along the polymer backbone will determine the polymer properties. Therefore, in this work, we focused on (i) establishing the synthetic pathway for generating soluble and solution-processable conjugated polymers of pyrazinacenes *via* condensation polymerization; (ii) varying the number of fused rings in pyrazinacene as well as substituents on the rings to study their impact on photophysical, and electrochemical properties, as a means to uncover the intricacies of extension of conjugation within the acene and along the chain.

2. Results and discussion

2.1 Synthesis of monomers

The nucleophilic aromatic substitution (S_NAr) reaction between dichlorodicyanopyrazine and aryl diamines is one of the efficient and quicker ways to generate pyrazinacenes containing multiple linearly fused pyrazine rings. A few hexaazapentacene-based pyrazinacenes have been synthesized through this approach by Miao and Hill groups.[39,44] However, none of these derivatives have solubilizing chains, so the self-condensation polymerization of these pyrazinacenes would result in insoluble oligomers beyond two repeat units. To impart solubility to the polymers, hexaazapentacene monomers containing four hexyloxy chains were synthesized as shown in Scheme 1. Installing hexyloxy chains onto the hexazaacene monomers has increased the required number of synthetic steps, but this is imperative to generate soluble polymers. Synthesis of the desired pyrazinacene monomers with pendant solubilizing

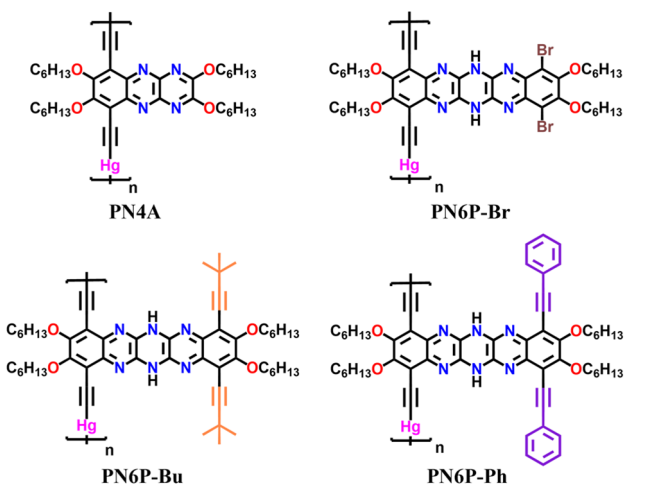

Fig. 1 Pyrazinacene polymers synthesized and studies in this work.

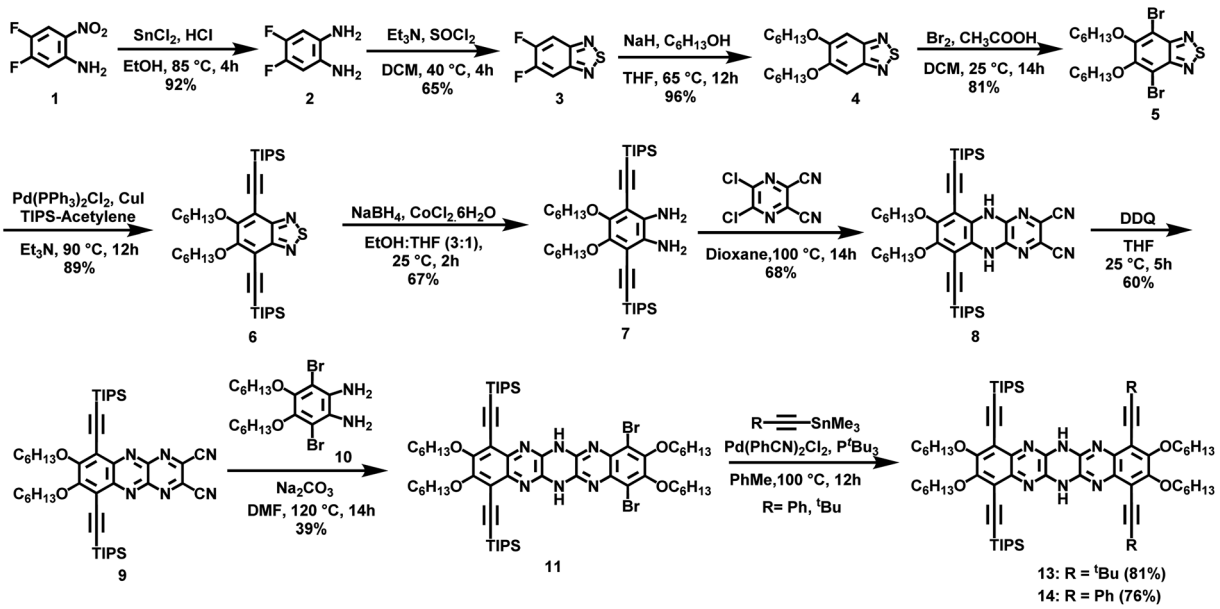

Scheme 1 Synthesis of TIPS protected pyrazinacene monomer precursors.

chains is synthetically challenging because chemical transformations of pyrazinacenes containing multiple linearly fused-pyrazine are highly structure specific; thus, synthesizing the desired monomers required screening of reaction conditions at a couple of synthetic steps (*vide infra*). Compounds **2–5** were synthesized following typical synthetic conditions reported for analogous compounds in the literature.[45–47] The Sonogashira coupling of dibromo dihexyloxy benzothiadiazole (**5**) with TIPS acetylene, followed by the reduction of thiadiazole resulted in the phenylene diamine compound **7**. Nucleophilic aromatic substitution reaction (S_NAr) by **7** onto 2,3-dichloro-5,6-dicyanopyrazine in 1,4-dioxane gave dihydrotetraazacenedicyano compound **8**. Oxidized **8** was subjected to another nucleophilic aromatic substitution reaction by dibromo dihexyloxy-phenylene diamine (**10**) to obtain the desired dihydrohexaazaacene compound **11** in 39% yield. The position of the hydrogens along the azaacene backbone can vary, giving rise to tautomers having different optical and electrochemical properties. Single crystal X-ray structure of **11** confirms that the hydrogens were on the middle pyrazine ring (Fig. S5†). Compound **11** was air-stable and did not oxidize to all pyrazine rings in the ambient atmosphere even though it contains an antiaromatic dihydropyrazine ring. This exceptional stability can be attributed to several factors, including the extended conjugation by the nitrogen lone pairs of the dihydropyrazine *via* enamine formation, an increased number of Clar rings, and delocalization of antiaromaticity. Desilylation of **11** gave the dialkynyl azaacene monomer N6P-Br in 68% yield. Attempts to oxidize the dihydropyrazine to pyrazine using PbO_2 was unsuccessful due to the electronic stabilization by delocalization and the presence of different substituents around N6P-Br. The bromo substituents on **11** were useful to functionalize the azaacenes further and generate electronically diverse monomers. With this in mind, **11** was subjected to various Sonogashira cross-coupling reaction conditions with trimethylsilylacetylene, which were unsuccessful (Table S1†). The Bunz[48,49] group have previously used Stille cross-coupling reactions to derivatize azaacenes. Taking cues from their work, **11** was subjected to Stille cross-coupling reaction with two alkynyl stannyl derivatives (R: *t*-Bu; Ph) in the presence of bis(benzonitrile)palladium(II) dichloride and P(*t*-Bu)$_3$ (Scheme 1). We were gratified to see that both derivatization reactions successfully resulted in azaacenes containing *t*-butyl acetylene (compound **13**) and phenyl acetylene (compound **14**). The observation that azaacenes were susceptible to Stille rather than Sonogashira cross-coupling indicated that the presence of amine base and/or Cu(I) salt in the Sonogashira coupling might have interfered with the hydrogens of the dihydropyrazine leading to no or undesired reaction. Desilylation of **13** and **14** gave two electronically diverse azaacene monomers, N6P-Bu and N6P-Ph (Scheme 2). Alkyne substituents in both these monomers are expected to extended π-conjugation of the acene.

To understand the effect of the number of fused rings in the azaacene repeat unit as well as the presence of the reduced pyrazine (dihydropyrazine) ring on the polymer's optical and electrochemical properties, compound **9** was used as comparison. **9** was subjected to a desilylation reaction using TBAF, but the starting material decomposed due to the strong nature of the fluoride source. Next, KF in the presence of $AgNO_3$ in MeOH/THF was used as a mild fluoride source for desilylation (Scheme 3). Surprisingly, this resulted in expected desilylation as well as unexpected nucleophilic aromatic substitution by methoxy groups at the carbons containing cyano groups (**17**). This unexpected outcome was leveraged to install two additional solubilizing pendant chains onto **9**, as shown in Scheme 3. For this, **9** was subjected to nucleophilic aromatic substitution reaction by hexyloxy groups to generate **18**, which was desilylated using KF/$AgNO_3$ to generate tetrazaanthracene dialkynyl monomer (N4A).

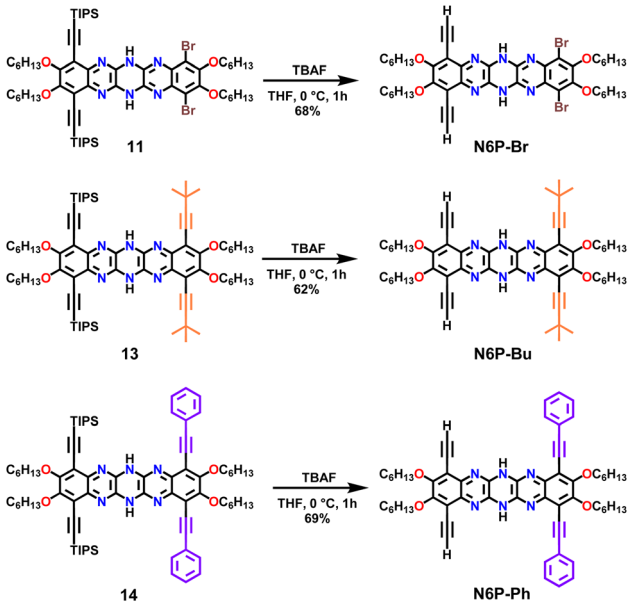

Scheme 2 Synthesis of pyrazinacene (hexaazapentacene) monomers.

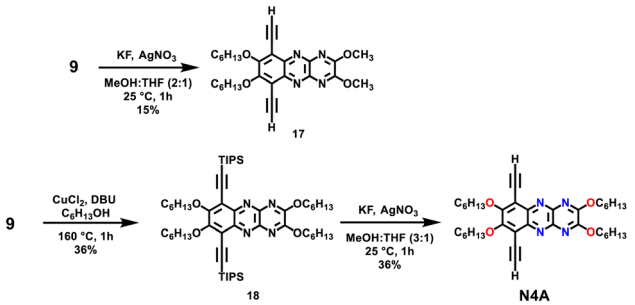

Scheme 3 Synthesis of tetrazaanthracene (N4A) monomer.

2.2 Synthesis of polymers

N6P-Br was used to optimize the polymerization conditions since its acene core is similar to the other two monomers (N6P-Bu and N6P-Ph) and requires two less synthetic steps. N6P-Br was subjected to Glaser–Hay polymerization because of its mild reaction conditions, but unfortunately, this resulted in only oligomers (Table 1). Synthesized azaacenes are air-stable; nonetheless, to see if the presence of oxygen in the reaction might be the reason for the lower degree of polymerization, the monomer was subjected to Eglinton[50] polymerization under nitrogen, but the reaction was unsuccessful. Continuing our efforts to replace oxygen, a modified Glaser–Hay polymerization conditions reported by the Swager[51] group that involved Pd(II) and Cu(I) catalysts and hydroquinone as an internal oxidant was tested (Table S2†). Unfortunately, the modified Glaser Hay polymerization conditions with the internal oxidant was also unsuccessful. Sonogashira polymerization of N6P-Br with diiodobenzene also did not yield any results. The limited success of the attempted polymerizations can be attributed to the presence of N–H protons on the dihydropyrazine ring of the pyrazinacene, which can interact with amine base and copper catalyst and interfere with the polymerization, similar to what we had observed for the Sonogashira cross-coupling of compound **11** with alkynes. To avoid polymerization reactions that involved amine base and copper, compound **11** was subjected to Stille condensation polymerization with bis(tributylstannyl) butadiyne[52] (Table S3†). To our surprise, even this reaction also resulted in only oligomers.

We scouted the literature for mild polymerization conditions for alkynes that do not involve amine base and Cu catalyst and result in conjugated polymers. Dehydrohalogenation–polymerization of the terminal diacetylenes with $HgCl_2$ in the presence of triethylamine to generate conjugated Hg(II) containing rigid rod polymetallynes caught our attention.[53,54] Mercury forms dicoordinated Hg(II) complexes (d^{10} configuration) with a linear geometry suitable for generating linear rigid rod conjugated polymers. A typical polymerization mechanism is shown in Scheme 4. The advantage of this reaction is that Hg(II) plays two roles: (i) it helps with the deprotonation of terminal acetylene similar to that of copper through eta complex, and (ii) it forms the σ-acetylide co-ordination compound with the terminal alkynes thus generating Hg(II) containing polymetallynes.[55–59] Several Hg(II) alkynyl small molecule complexes and a few polymers have been synthesized through a dehydrohalogenation approach by reacting Hg(II) halide precursors and active terminal alkynes in the presence of a base.[53,54,58,60] Both experimental and theoretical studies have shown that the mercury metal center is involved in extending the π-delocalization along the polymer backbone. A handful of Hg(II) containing conjugated polymetallynes have been synthesized to take advantage of the dπ–pπ conjugation and the resultant spin–orbit coupling between the mercury and organic spacer to generate highly phosphorescent polymers.[58] Since this polymerization does not require a copper catalyst and generates Hg(II) containing small molecule complexes and polymers in good yield at room temperature, these polymerization conditions were tested on pyrazinacenes. It is gratifying to report that the polymerization of N6P-Br in the presence of $HgCl_2$, triethylamine, in a mixture of DCM and MeOH gave organometallic conjugated pyrazinacene polymer (PN6P-Br) with a decent number average molecular weight (14 kDa).

The effect of the amine base on polymerization was screened by changing the amine base and keeping the other reaction conditions the same (Table 2). All the studied amines except pyridine gave similar molecular weight polymers (M_n: *ca.* 11 kDa), whereas pyridine gave a lower molecular weight polymer (M_n: 9 kDa). Next, triethylamine was kept as the amine, and the equivalence of $HgCl_2$ was changed from 0.5 to 1.5 equivalents with respect to the dialkyne monomer (Table 3). The change in the degree of polymerization as the reactant's stoichiometric ratio is varied does not follow the step-growth polymerization model. The seminal Carothers equation shows that a strict stoichiometry of monomers (A_2 and B_2) is required for a step-growth polymerization to realize high molecular weight polymers. A slight imbalance in the stoichiometry leads to a drastic reduction in the polymer molecular weight. Excess monomer present in the polymerization mixture ends up as a terminal

Table 1 Attempted alkyne–alkyne coupling polymerization conditions[b]

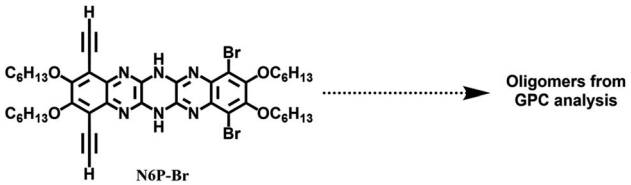

Entry	[Cu]	Base	Solvent	Temp. (°C)	Time (h)
1	CuCl	TMEDA[a]	CH_2Cl_2	35	48
2	CuCl	TMEDA[a]	PhMe : ACN (2 : 1)	55	24
3	$Cu(OAc)_2$	Pyridine	PhMe	25	24
4	CuCl, $CuCl_2$	Pyridine	CH_2Cl_2	25	7
5	CuCl, $CuCl_2$	Pyridine	$CHCl_3$	50	4

[a] TMEDA: tetramethylethylenediamine. [b] All reactions were performed with 15 mg of N6P-Br (1 eq.), Cu-source (2 eq.), base (6 eq.) in 1.8 mL of solvent.

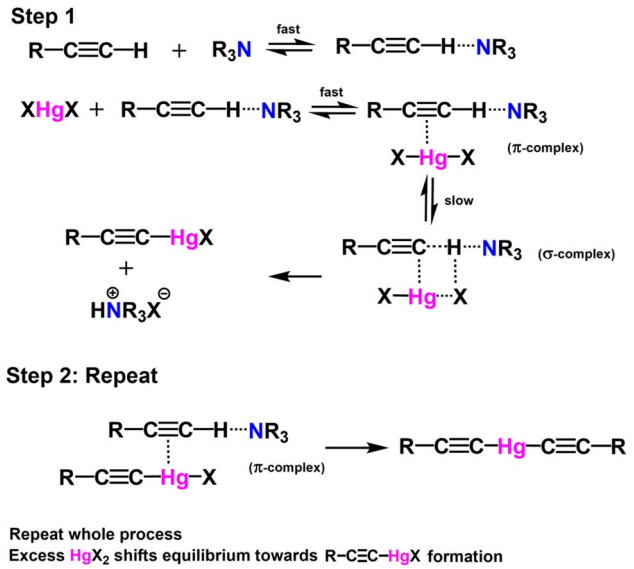

Scheme 4 Typical dehydrohalogenation reaction mechanism of terminal alkynes with $HgCl_2$.

group, thus hindering further condensation of growing chains resulting in low molecular weight polymers/oligomers. Contrary to that, polymer molecular weight increased with the increase in $HgCl_2$ equivalence until 1.25 and reached a plateau. The key reason for the difference between conventional step-growth polymerization and $HgCl_2$ containing organometallic polymerization is that the RHgCl self-condenses to generate R_2Hg and $HgCl_2$.[56,57] The concentration of RHgCl increases in the reaction mixture with the increase in $HgCl_2$ equivalence; RHgCl can react with terminal alkyne as shown in Scheme 4 to generate dialkynylmercury, which will elongate the polymer chain. Alternatively, two RHgCl molecules can self-react to generate dialkynylmercury (RHgR) and $HgCl_2$ as shown in Scheme 5, which will also elongate the polymer chain and regenerate the ($HgCl_2$) monomer respectively.

In order to have better control over resultant polymer molecular weight and soluble polymer yield, optimized polymerization conditions (triethylamine, methanol, and DCM as solvents in a 1 : 1 : 3 ratio and 1 equivalent of $HgCl_2$) were used for all the four monomers (Scheme 6). The polymerization mixture was concentrated, precipitated in methanol, and filtered. The crude polymer was subjected to soxhlation with methanol for all polymers. Diethyl ether was used as the second purification solvent for PN6P-Br and PN4A, whereas acetonitrile was used as the second purification solvent for PN6P-Bu and PN6P-Ph. The precipitate left in the thimble was dried and used for characterization. The synthesized polymers were soluble in typical organic solvents used for conjugated polymers, such as tetrahydrofuran, chloroform, and dichlorobenzene. The polymer molecular weights were determined using gel permeation chromatography (tetrahydrofuran as the eluent) against polystyrene standards. The number average molecular weights of the copolymers are in the range of 15 to 22 kDa.

2.3 UV-vis absorption and emission properties

An increase in the number of fused rings from three (N4A) to five (N6P-series) has increased the absorption maximum of monomers by *ca.* 100 nm (Table 4). This trend is also observed in the polymers as well, the absorption maximum of hexaazapentacene polymers (PN6Ps: PN6P-Br, PN6P-Bu, PN6P-Ph) is *ca.* 100 nm red-shifted compared to tetraazaanthracene polymer (PN4A). This suggests that even though the middle dihydropyrazine ring is formally antiaromatic ($4n\pi$ electrons), it does not isolate hexazapentacene into two electronically independent halves, each containing quinoxalines. Moreover, both the absorption and emission spectra of hexaazapentacene monomers show a fine structure typically observed in acenes,[42] which also supports the extended conjugation in the acene through the dihydropyrazine (Fig. 2). Bunz group and others have suggested that the azaacenes containing dihydropyrazines exhibit enamine conjugations involving the nitrogen lone pairs of dihydropyrazine. Also, using nucleus-independent chemical

Table 2 Amine base optimization for dehydrohalogenation polymerization[a]

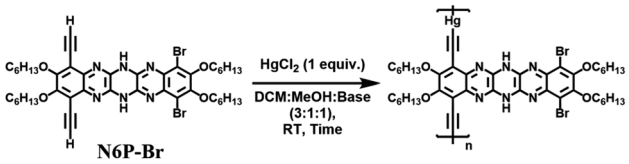

Entry	Base	Time (h)	M_n/M_w (kDa)	X_n/X_w	$Đ$
1	Diisopropylamine	1	12/18	11/16	1.5
2	Tetramethylethylenediamine	1	11/14	10/13	1.2
3	Diisopropylethylamine	1	12/18	11/16	1.5
4	Pyridine	1	9/11	8/10	1.2
5	Piperidine	1	11/16	10/15	1.4
6	Triethylamine	1	14/21	13/19	1.5

[a] Where M_n is the number average molecular weight, M_w is the weight average molecular weight, X_n is number average degree of polymerization, X_w is weight average degree of polymerization and $Đ$ is the polydispersity index. All reactions were performed with 10 mg of N6P-Br (1 eq.) at RT. All GPCs were reported after washing with MeOH/diethyl ether. Polymer molecular weights were determined using gel permeation chromatography (tetrahydrofuran as the eluent) against polystyrene standards.

Table 3 $HgCl_2$ equivalents optimization for dehydrohalogenation polymerization[a]

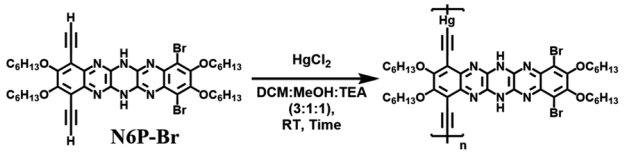

Entry	$HgCl_2$ (equiv.)	Time (h)	M_n/M_w (kDa)	X_n/X_w	$Đ$
1	0.50	1	8/13	7/12	1.2
2	0.75	1	14/25	13/23	1.8
3	1.0	1	14/21	13/19	1.5
4	1.25	1	20/45	18/41	2.3
5	1.50	1	19/31	17/28	1.6

[a] Where M_n is the number average molecular weight, M_w is the weight average molecular weight, X_n, is number average degree of polymerization, X_w, is weight average degree of polymerization and $Đ$ is the polydispersity index. All reactions were performed with 10 mg of N6P-Br (1 eq.) at RT. All GPCs were reported after washing with MeOH/diethyl ether. Polymer molecular weights were determined using gel permeation chromatography (tetrahydrofuran as the eluent) against polystyrene standards.

shift calculations it has been shown that the antiaromaticity in these azaacenes is reduced due to delocalization.[43] Thus, the dihydropyrazine in the hexaazapentances, even though it is in the reduced form, extends the conjugation across the hexaazaapentance resulting in higher UV-vis absorption maximum. Within the hexaazapentacene monomers, installing *t*-butylacetylene and phenylacetylene in the place of bromide has slightly red-shifted the absorption maximum due to extension of π-conjugation. The absence of significant changes to the absorption peak pattern indicates that the hexaazaacene core is still the effective chromophore in these substrates and the alkynyl substituents have minimal effect on the major electronic transitions.

All the hexaazapentacene monomers showed clear vibronic transitions but upon polymerization the absorption spectra became broader with less defined vibronic transitions. Even though the absorption maximum of PN6Ps is near the corresponding monomers, the polymers have an ill-defined vibronic transition in the red-region of the spectra (*ca.* 530 and 580 nm) (Fig. 2). This indicates that the π-electrons of azaacene repeat unit can delocalize beyond a single repeat unit and confirms the extension of π-conjugation along the polymer backbone through the metal center. Thus, Hg(II), albeit weaker than the conventional fully organic backbone, extends the π-conjugation along the polymer backbone. Emission spectra of hexaazapentacenes is approximately a mirror image of the UV-vis

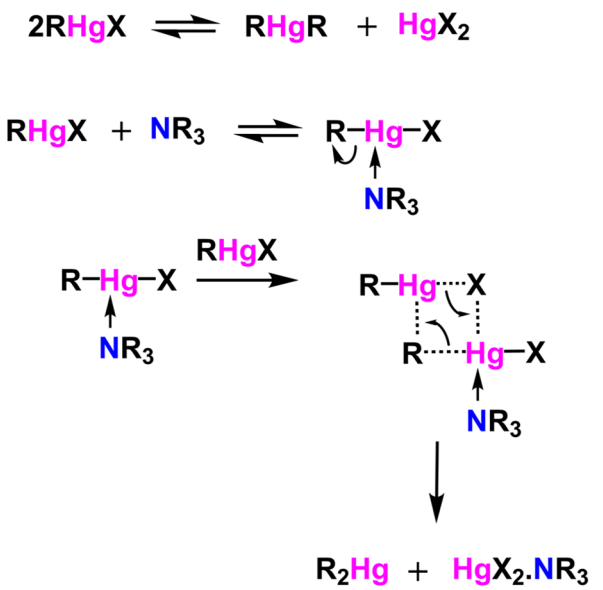

Scheme 5 Typical self-condensation reaction of organomercury intermediate (RHgCl) into R_2Hg and $HgCl_2$.

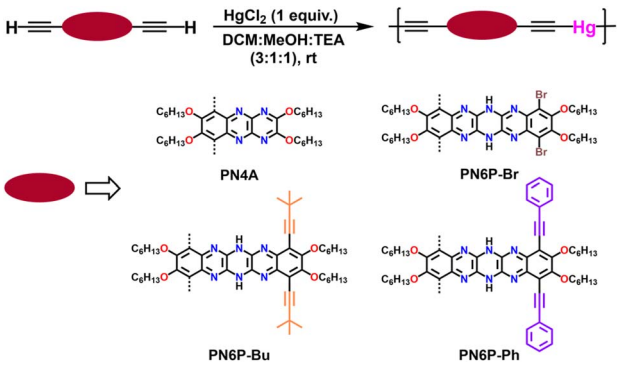

Scheme 6 Synthesis of pyrazinacene polymers using dehydrohalogenation polymerization with $HgCl_2$.

absorption spectra with very small Stokes shift (*ca.* 10 nm) typically observed in rigid molecular frameworks having acene-type structures. Both the alkyne and hexyloxy substituents on N4A have a significant effect on the N4A absorption and emission spectra. Unlike hexaazapentacene monomers, N4A has broad peaks in both absorption and emission spectra and displayed *ca.* 140 nm Stokes shift. The deviation from typical acene-like optical transitions in N4A indicates that the effective chromophore responsible for optical transitions in N4A has extended beyond the acene core. The emission spectra of PN4A and PN6Ps is similar to that of corresponding monomers.

A significant advantage of the dihydrohexaazaapentacenes is that the acidic protons on the reduced pyrazine ring bestows anion-dependent UV-vis absorption and emission properties compared to the oxidized tetrazaanthracene. The impact of F^- and OH^- anions on the UV-vis absorption and emission properties of monomers and polymers are studied. In the presence of both these anions, all the dihydrohexaazaapentancene monomers and polymers showed significant changes to the UV-vis absorption (Fig. 3). Whereas, fully oxidized tetrazaanthracene monomer and polymer showed no significant changes to the UV-vis absorption properties in the presence of studied anions confirming that: (i) the NH protons are responsible for observed spectral shifts; and (ii) interaction of anions with the Hg(II), if it exists, is not the reason for the observed spectral changes. In general, the introduction of F^-, and OH^- anions into the PN6Ps solution suppressed the intensity of the existing peaks (parent peaks) and three new major vibronic transitions (range: 500–600 nm) appeared in the red-region of the spectra. Polymer solutions change color from yellow to pink or purple depending on the polymer and ions added. The spectral changes *i.e.*, the amount of suppression of parent peaks and the intensity of the new transitions are higher for OH^- compared to F^-. The spectral shifts are generally associated with the deprotonation of dihydropyrazine NH protons in the presence of F^- or OH^-. Similar shifts and color changes have been reported for the monoanion formation in pyrazines.[36] The deprotonated PN6Ps are stable against oxidation by ambient oxygen (purging with air) and persist in solution. The formation of a nonsymmetric diamagnetic Meisenheimer complex/C–F bond *via* a nucleophilic attack[61] was ruled out as the shift in UV-Vis spectra could be reversed back to the original state after work-up with water. Emission spectra of dihydrohexaazapentacenes monomers and polymers in the presence of F^- and OH^- shifted from the parent emission peak by 80 to 100 nm similar to that of UV-Vis absorption peaks (Fig. S9 and S11†). PN4A showed no new emission peaks in the presence of studied anions instead the intensity of the emission peak is suppressed.

2.4 Cyclovoltammetry and DFT-B3LYP simulations

Cyclic voltammetry of polymers and monomer-precursors is performed (Fig. 4) to understand the role of Hg(II) on polymers electrochemistry and obtain frontier orbital energy levels. Alkyne-protected monomers *i.e.*, monomer-precursors (**11**, **13**, **14**, and **18**) are used instead of monomers for electrochemical studies to avoid undesired electrochemical reactions. Electrochemical properties are affected by the number of pyrazine units and the substituents. All the small molecules and polymers did not show any oxidation peaks highlighting the electron deficient nature of the azaacenes studied here. Unlike the UV-vis absorption data the N4A-precursor (**18**), which contains lower number of fused rings than the hexaazaacene-precursors (**11**, **13** and **14**), reduces at smaller negative potentials highlighting the importance of presence of fully oxidized pyrazines over hexaazapentacenes with a dihydropyrazine for accepting

Table 4 Comprehensive optical properties of polymers and monomers[a]

Polymer/monomer	M_n/M_w (kDa)	X_n/X_w	Yield[b] (%)	λ_{max}^{abs} THF (nm)	λ_{ex}[c] (nm)	λ_{max}^{em} THF (nm)	Stokes shift (nm)
PN4A	22/35	26/38	94	386	386	527	141
N4A				388	390	481	93
PN6P-Br	15/37	14/34	89	458	437	480	22
N6P-Br				470	442	479	9
PN6P-Bu	21/36	19/33	93	474	455	488	14
N6P-Bu				477	450	487	10
PN6P-Ph	20/36	18/32	90	485	460	496	11
N6P-Ph				485	455	495	10

[a] Where M_n is the number average molecular weight, M_w is weight average molecular weight, X_n is number average degree of polymerization and X_w is weight average degree of polymerization. Polymer molecular weights were determined using gel permeation chromatography (tetrahydrofuran as the eluent) against polystyrene standards. [b] After Soxhlet extraction. [c] Excitation wavelength for reported emission spectra.

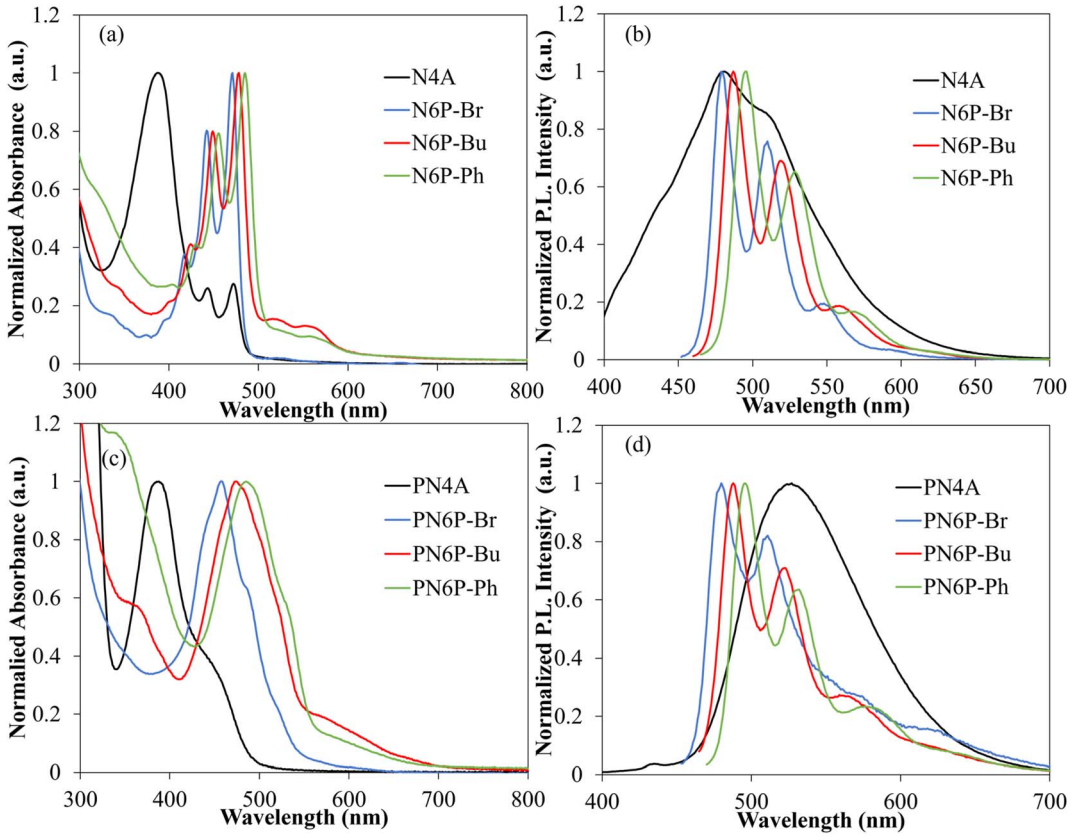

Fig. 2 Normalized UV-Vis absorption and emission spectra of monomers (a and b) and polymers (c and d) in tetrahydrofuran. Excitation wavelengths are reported in Table 2.

electrons. The N4A-precursor, without the dihydropyrazine ring, show two well-defined quasi reversible reduction peaks, while the hexaazacene-precursors containing a dihydropyrazine ring undergo reduction at larger negative potentials. The hexaazapentacene-precursors showed a clear substitution-dependent electrochemical behavior. N6P-Bu-precursor (**13**) and N6P-Ph-precursor (**14**) showed two reduction peaks similar to that of N4A-precursor (**18**) but at slightly larger negative potentials. On the other hand, the N6P-Br-precursor (**11**) showed only one reduction peak at a potential similar to that of N6P-Ph-precursor. The presence of two (oxidized) pyrazine rings in the N4A precursor make it more electron deficient, help stabilize the FMOs and favor redox process at lower negative potential. Whereas the lone pair of electrons on the nitrogens of the reduced dihydropyrazine make hexaazapentacenes electron rich *via* enamine conjugation, thus destabilizing the FMOs and pushing the reduction potentials to larger negative potentials. Simulations of molecular orbitals provide relative energy levels and help in understanding the electronic structure of the repeat units. More importantly, DFT simulations provide a detailed account of the distribution of the electron density of the orbitals across the repeat units including the metal center (Fig. 5). In order to rationalize the electrochemical reduction behavior, frontier molecular orbitals of monomers and dimers (containing one Hg(II) at the center) are simulated (Fig. 6, S13 and S14†). The molecular geometries were optimized using density functional theory (DFT at genecp level, Stuttgart RSC 1997 ECP was used for Hg, and B3LYP/6-311g(d,p) was used for all other atoms). Indeed, the simulated FMOs of N4A are more stabilized than the hexaazaacenes. The LUMO of N4A has the electron density distributed across all the pyrazine nitrogens, whereas the nitrogens in the middle pyrazine ring of hexaazapentacene monomers have no electron density and act as nodal points. The difference in the distribution of electron density along the azaacenes stem from the oxidation state of pyrazine rings and could be the reason for lower reduction potentials of N4A. Within the hexaazapentacene monomers, installing *t*-butylacetylene and phenylacetylene in the place of bromide has further extended the electron delocalization of acene core in the LUMO of N6P-Bu and N6P-Ph, possibly facilitating two redox processes in the alkyne substituents containing substrates. It is worth noting that the LUMOs of the hexaazapentacene precursors are higher than that of similar azaacene compounds reported in the literature, showing that the addition of different substituents, including alkoxy substituents, significantly affects the electron affinity.[44,62,63]

As a pleasant surprise, contrary to what has been observed in monomers, the hexaazaacene polymers (PN6Ps) showed reduction waves at smaller negative potentials than the PN4A without any reduced pyrazine rings (Table 5). PN6Ps retained the electrochemical behavior observed in monomer-precursors. All the PN6Ps, including the PN6P-Br, showed

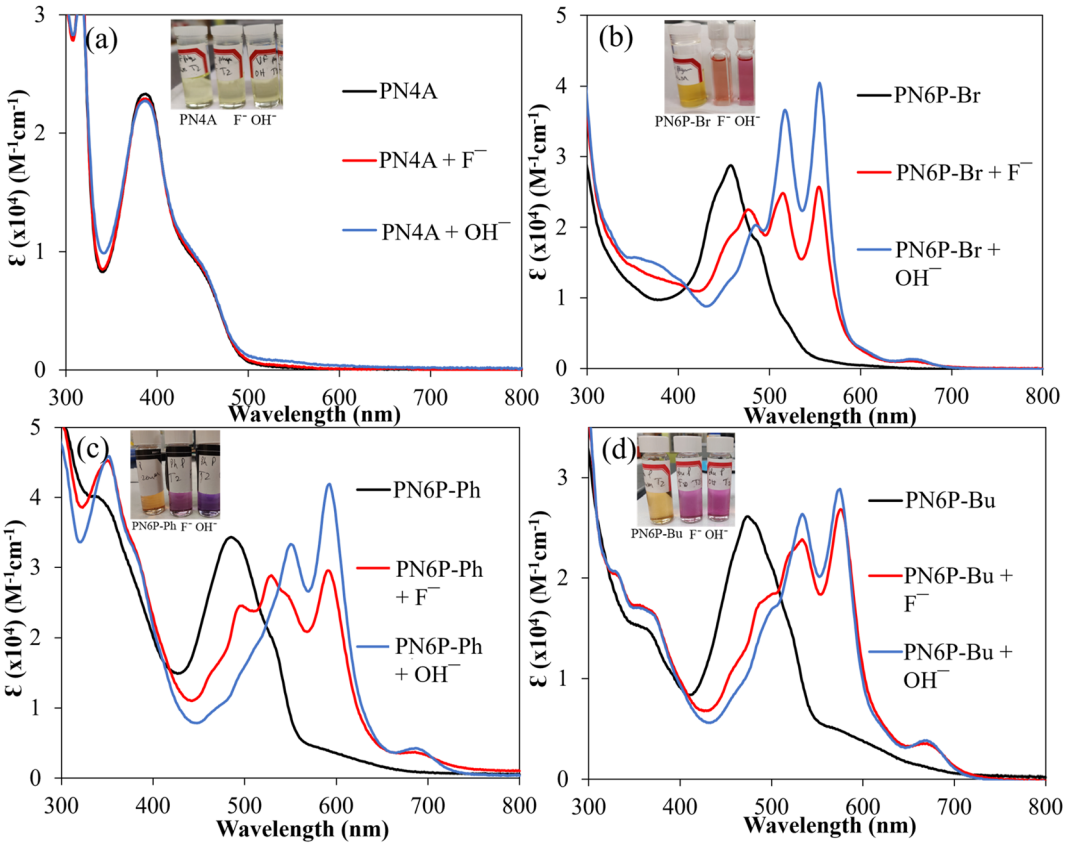

Fig. 3 UV-vis absorption spectra of polymers before and after the addition of 10 equivalents of fluoride and hydroxide anions in tetrahydrofuran recorded after 30 min of anion addition (inset shows color change of solutions after addition of anions).

two reduction peaks. More importantly, a remarkable drop in the reduction potentials by *ca.* 2 eV for hexaazapentacenes upon polymerization indicates that the Hg(II) is playing a significant role in altering the redox properties of polymers and stabilizing the reduced species (Table 5). Moreover, PN6P-Ph showed relatively better redox peaks than the corresponding monomer and other two hexaazapentacene polymers (PN6P-Br and PN6P-Bu). Surprisingly, the reduction potential dropped only by 0.2 eV for tetraazaanthracene upon polymerization. In order to understand for such a significant drop in reduction potentials, simulations are performed on the dimers containing the Hg(II) metal at the center. HOMO of the dimers has no significant electron density on the metal center. On the other hand, LUMO of the hexaazapentacene dimers has electron density on the metal center as well as on the acene. Whereas the LUMO of the tetrazaanthracene dimer has no significant electron density on the metal center. This is also evident in the change in frontier orbital energy levels of dimers compared to that of monomers (Fig. 6, S13 and S14†). Mostly, the LUMOs of hexaazaapentacene dimers are affected due to the incorporation of metal center. This indicates that metal center facilitates the conjugation of hexaazapentancene LUMOs along the polymer backbone but not for the tetrazaanthracene. As a result, the LUMO of PN6Ps is extended along the polymer backbone through the metal centers. The extension of the electron density through the Hg(II) bridge in the LUMOs helped PN6Ps to significantly lower the reduction potential by *ca.* 2 eV. And the absence of such extension through Hg(II) bridge in PN4A lowered the reduction potential by only *ca.* 0.2 eV. Mulliken population analysis showed that the Hg(II) does not contribute to the LUMO orbitals of the Hg(II) bridged N4A dimer and indeed the spatial distribution of the LUMO orbital showed no electron density on the Hg(II) bridge. Whereas the Mulliken population analysis of Hg(II) bridged hexazapentacenes indicated 5%, 6% and 4% electron density on the Hg(II) center for N6P-Br, N6P-Bu, and N6P-Ph dimers respectively (Fig. S12†). Within the hexaazapentacenes the phenyl acetylene substituents stabilize the reduced species through extended conjugation giving rise to relatively reversible reduction waves. Thus, the pπ orbital interactions of the metal and hexaazapentacene provides a pathway for the delocalization of electron density along the polymer backbone and facilitate electrochemical reduction at lower negative potential. The electrochemical studies have unveiled a pivotal molecular design principle, the presence of dihydropyrazine (reduced pyrazines) reduces the extension of π-conjugation within the pyrazinacene but propitiously this allows the extension of electron density between the repeat units through the Hg(II) metal bridge and lowers the LUMO energy level. Simulations of the singly occupied molecular orbitals (SOMO) of dimers indicated that the odd electron is fully delocalized throughout the dimer including the metal

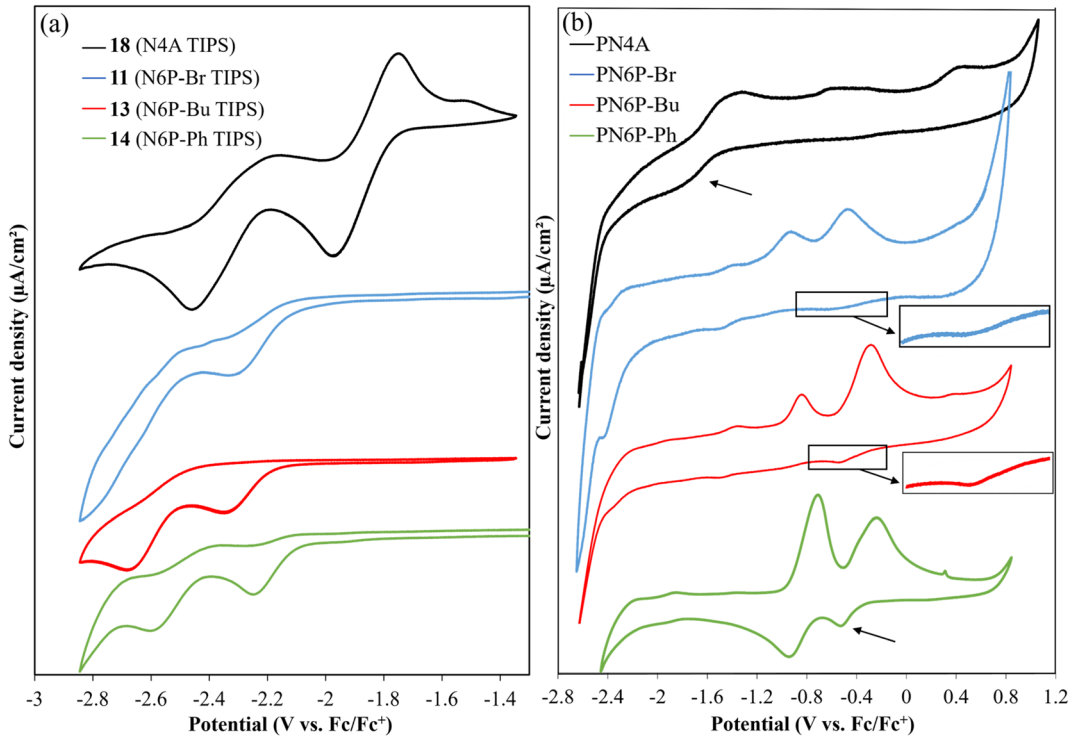

Fig. 4 Cyclic voltammograms of monomer precursors (left) and polymers (right). Glassy carbon, platinum wire, and Ag/Ag^+ wire (0.01 M $AgNO_3$ in 0.1 M $TBAPF_6$ solution of MeCN) were used as working, counter, and reference electrodes respectively. Monomer precursors were dissolved in 0.1 M $TBAPF_6$ solution of THF and polymer films were drop coated onto glassy carbon electrode and immersed in 0.1 M $TBAPF_6$ solution of MeCN.

center (Fig. 7). Since the monomer-precursors and polymers did not exhibit any oxidation potentials, the HOMO values were calculated using the optical band gap obtained from thin film UV-Vis absorption band red-edge (see Fig. S8†). Electrochemical studies of the control molecules (diphenylethynylmercury, and $HgCl_2$) confirm that the observed redox peaks in polyazaacenes are arising from the polymer backbone as a result of conjugation between azaacene and Hg(II) and not from the Hg(II) center alone (see ESI Fig. S19 and S20† for the control molecules cyclic voltammetry data).

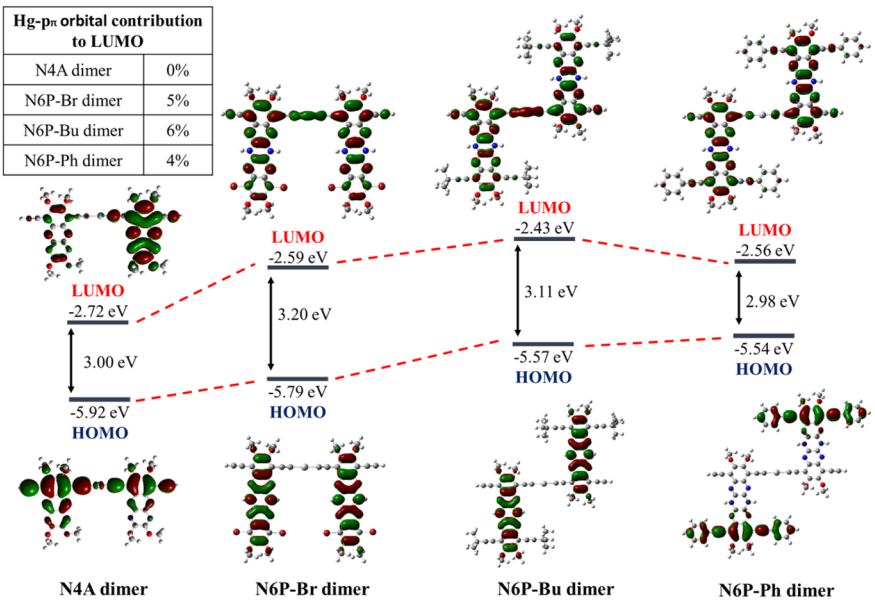

Fig. 5 DFT-B3LYP simulated HOMO and LUMO orbitals of dimers and the inset shows the Hg(II) pπ orbital contribution to the LUMO of the dimers.

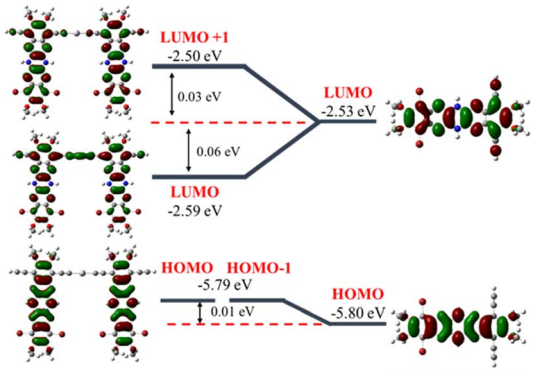

Fig. 6 DFT-B3LYP simulations of frontier molecular orbitals of N6P-Br monomer (right) and dimer (left) to compare the change in HOMO and LUMO energy levels upon bridging the monomers through Hg(II).

Table 5 Electrochemical properties of polymers and monomer-precursors

Polymer/TIPS monomer	E_g^{opt} [a] (eV)	LUMO^{CV} [b] (eV)	HOMO^{UV} [c] (eV)
PN4A	2.31	−3.27	−5.40
18 (N4A TIPS)	2.85	−3.02	−5.87
PN6P-Br	2.17	−4.68	−6.85
11 (N6P-Br TIPS)	2.54	−2.70	−5.24
PN6P-Bu	2.13	−4.50	−6.63
13 (N6P-Bu TIPS)	2.50	−2.62	−5.12
PN6P-Ph	2.21	−4.42	−6.63
14 (N6P-Ph TIPS)	2.45	−2.70	−5.15

[a] From onset of thinfilm UV-Vis absorption spectra. [b] From reduction peak onset in CV. [c] HOMO^{UV} calculated from E_g^{opt} − LUMO^{CV} values.

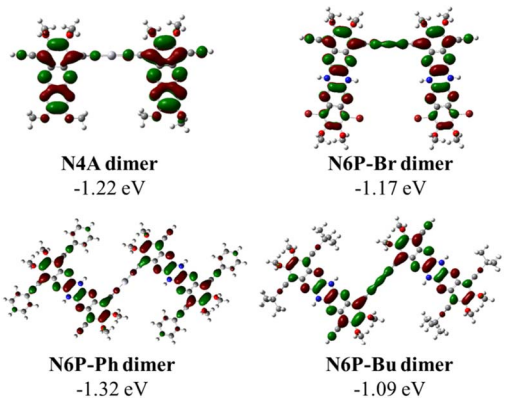

Fig. 7 DFT-B3LYP simulated SOMOs of radical anions of dimers.

3. Conclusions

In summary, we successfully overcame the synthetic challenges associated with the polymerization of pyrazinacenes, resulting in the generation of a series of highly sought-after and elusive pyrazinacene polymers, nearly a century after their initial discovery. The key strategies behind this successful synthesis included the design of pyrazinacene monomers that would yield solution-soluble conjugated polymers and the identification of a Pd and Cu-free dehydrohalogenation polymerization method. Achieving these milestones required the optimization and establishment of several synthetic steps within the 12-step synthetic pathway and screening the polymerization of pyrazinacene monomers using various Pd and Cu-catalyzed methods. Gratifyingly, pyrazinacenes undergo Pd and Cu-free dehydrohalogenation polymerization with $HgCl_2$, resulting in high molecular weight organometallic conjugated pyrazinacene polymers within just a few minutes at room temperature. The dual role played by Hg(II) during the polymerization, coupled with the self-coupling of the RHgCl intermediates, lies at the core of this successful polymerization process. Notably, the self-coupling of intermediates challenges the strict stoichiometric balance typically required for step-growth polymerization. Thus, $HgCl_2$, unlike other popular transition metal halides (such as $PdCl_2L_2$ and $PtCl_2L_2$), offers a novel step-growth polymerization method to generate high molecular weight organometallic conjugated polymers without the need for strict monomer stoichiometry. A combination of electrochemical studies and DFT-B3LYP simulations revealed that the presence of reduced pyrazine rings (*i.e.*, NH protons) promotes interacene π-conjugation through the metal center, in contrast to completely oxidized tetrazaazaanthracene. In terms of molecular design principles, although dihydropyrazine reduces the extension of π-conjugation within the pyrazinacene, it extends the conjugation along the polymer backbone and lowers the LUMO energy level. This extended conjugation results in an approximately 2 eV lower reduction potential for the polymers compared to the monomeric unit, placing the LUMO energy levels within the range of −4.68 to −4.42 eV for these polymers, which is comparable to some of the best-known n-type polymers.[64–67] Therefore, pyrazinacene conjugated polymers offer a straightforward strategy for generating n-type polymers with low-lying LUMOs capable of undergoing multi-electron reduction. These pyrazinacene polymers hold great promise across a wide range of applications, including organic electronics, energy conversion and storage, electrochemical transistors, catalysis, and sensors.[68–75] Additionally, they help to narrow the gap between number of p-type and n-type polymers.

Data availability

Synthesis and characterization details of small molecules and polymers are included in the experimental ESI.† Simulation details for dimers and small molecules are provided in the simulations ESI.†

Author contributions

F. H., A. M. and V. S. F. performed the synthesis of monomers and polymers. F. H. performed the structural and optical characterizations, simulations and was involved in the draft writing. N. G. conceived the idea, guided the experimental work, involved in the data analysis, and prepared the manuscript.

Conflicts of interest

There are no conflicts of interest to declare.

Acknowledgements

This work was supported by a National Science Foundation CAREER Grant (NSF-1944184) and Georgetown University. V. S. F. acknowledges the Georgetown University-Institute for Soft Matter Synthesis and Metrology Graduate Student Fellowship. We would like to thank Prof. Miklos Kertesz and Dr Rameswar Bhattacharjee for help pertaining to computations with density functional theory and Dr Jeffery A. Bertke for performing the single crystal X-ray Diffraction and analysis.

References

1 T. Dallos, D. Beckmann, G. Brunklaus and M. Baumgarten, Thiadiazoloquinoxaline–Acetylene Containing Polymers as Semiconductors in Ambipolar Field Effect Transistors, *J. Am. Chem. Soc.*, 2011, **133**(35), 13898–13901.

2 S. Wang, M. Kappl, I. Liebewirth, M. Müller, K. Kirchhoff, W. Pisula and K. Müllen, Organic field-effect transistors based on highly ordered single polymer fibers, *Adv. Mater.*, 2012, **24**(3), 417–420.

3 P.-L. T. Boudreault, J.-F. Morin and M. Leclerc, Synthesis of poly (2, 7-carbazole) s and derivatives, *Des. Synth. Conjugated Polym.*, 2010, 205–226.

4 F. Garnier, R. Hajlaoui, A. Yassar and P. Srivastava, All-polymer field-effect transistor realized by printing techniques, *Science*, 1994, **265**(5179), 1684–1686.

5 M. He, J. Li, M. L. Sorensen, F. Zhang, R. R. Hancock, H. H. Fong, V. A. Pozdin, D.-M. Smilgies and G. G. Malliaras, Alkylsubstituted thienothiophene semiconducting materials: structure– property relationships, *J. Am. Chem. Soc.*, 2009, **131**(33), 11930–11938.

6 R. J. Kline, M. D. McGehee, E. N. Kadnikova, J. Liu and J. M. Frechet, Controlling the field-effect mobility of regioregular polythiophene by changing the molecular weight, *Adv. Mater.*, 2003, **15**(18), 1519–1522.

7 M. Leclerc and J.-F. Morin, *Design and synthesis of conjugated polymers*, John Wiley & Sons, 2010.

8 D. Lehnherr, J. Gao, F. A. Hegmann and R. R. Tykwinski, Pentacene-based dendrimers: synthesis and thin film photoconductivity measurements of branched pentacene oligomers, *J. Org. Chem.*, 2009, **74**(14), 5017–5024.

9 H. Sirringhaus, Device physics of solution-processed organic field-effect transistors, *Adv. Mater.*, 2005, **17**(20), 2411–2425.

10 S. Sivaramakrishnan, P.-J. Chia, Y.-C. Yeo, L.-L. Chua and P. K.-H. Ho, Controlled insulator-to-metal transformation in printable polymer composites with nanometal clusters, *Nat. Mater.*, 2007, **6**(2), 149–155.

11 H. N. Tsao, D. Cho, J. W. Andreasen, A. Rouhanipour, D. W. Breiby, W. Pisula and K. Müllen, The influence of morphology on high-performance polymer field-effect transistors, *Adv. Mater.*, 2009, **21**(2), 209–212.

12 H. Yan, Z. Chen, Y. Zheng, C. Newman, J. R. Quinn, F. Dötz, M. Kastler and A. J. N. Facchetti, A high-mobility electron-transporting polymer for printed transistors, *Nature*, 2009, **457**(7230), 679–686.

13 M. Zhang, H. N. Tsao, W. Pisula, C. Yang, A. K. Mishra and K. Müllen, Field-effect transistors based on a benzothiadiazole– cyclopentadithiophene copolymer, *J. Am. Chem. Soc.*, 2007, **129**(12), 3472–3473.

14 B. Purushothaman, S. R. Parkin and J. E. Anthony, Synthesis and stability of soluble hexacenes, *Org. Lett.*, 2010, **12**(9), 2060–2063.

15 X.-Z. Bo, N. Tassi, C. Lee, M. Strano, C. Nuckolls and G. B. Blanchet, Pentacene-carbon nanotubes: Semiconducting assemblies for thin-film transistor applications, *Appl. Phys. Lett.*, 2005, **87**(20), 203510.

16 T. Okamoto and Z. Bao, Synthesis of solution-soluble pentacene-containing conjugated copolymers, *J. Am. Chem. Soc.*, 2007, **129**(34), 10308–10309.

17 T. Okamoto, Y. Jiang, F. Qu, A. C. Mayer, J. E. Parmer, M. D. McGehee and Z. Bao, Synthesis and Characterization of Pentacene- and Anthradithiophene- Fluorene Conjugated Copolymers Synthesized by Suzuki Reactions, *Macromolecules*, 2008, **41**(19), 6977–6980.

18 S. K. Park, T. N. Jackson, J. E. Anthony and D. A. J. A. P. L. Mourey, High mobility solution processed 6, 13-bis (triisopropyl-silylethynyl) pentacene organic thin film transistors, *J. Appl. Phys.*, 2007, **91**(6), 063514.

19 W. Fudickar and T. Linker, Why triple bonds protect acenes from oxidation and decomposition, *J. Am. Chem. Soc.*, 2012, **134**(36), 15071–15082.

20 A. Maliakal, K. Raghavachari, H. Katz, E. Chandross and T. Siegrist, Photochemical stability of pentacene and a substituted pentacene in solution and in thin films, *Chem. Mater.*, 2004, **16**(24), 4980–4986.

21 E. Kumarasamy, S. N. Sanders, A. B. Pun, S. A. Vaselabadi, J. Z. Low, M. Y. Sfeir, M. L. Steigerwald, G. E. Stein and L. M. Campos, Properties of Poly- and Oligopentacenes Synthesized from Modular Building Blocks, *Macromolecules*, 2016, **49**(4), 1279–1285.

22 C. L. Anderson, T. Zhang, M. Qi, Z. Chen, C. Yang, S. J. Teat, N. S. Settineri, E. A. Dailing, A. Garzon-Ruiz, A. Navarro, Y. Lv and Y. Liu, Exceptional Electron-Rich Heteroaromatic Pentacycle for Ultralow Band Gap Conjugated Polymers and Photothermal Therapy, *J. Am. Chem. Soc.*, 2023, **145**(9), 5474–5485.

23 J. Kim, A.-R. Han, J. H. Seo, J. H. Oh and C. J. C. o. M. Yang, β-Alkyl substituted Dithieno [2, 3-d; 2′, 3′-d′] benzo [1, 2-b; 4, 5-b′] dithiophene Semiconducting Materials and Their Application to Solution-Processed Organic Transistors, *Chem. Mater.*, 2012, **24**(17), 3464–3472.

24 B. Cirera, A. Sánchez-Grande, B. de la Torre, J. Santos, S. Edalatmanesh, E. Rodríguez-Sánchez, K. Lauwaet, B. Mallada, R. Zbořil and R. J. N. n. Miranda, Tailoring topological order and π-conjugation to engineer quasi-metallic polymers, *Nat. Nanotechnol.*, 2020, **15**(6), 437–443.

25 G. Li, Y. Wu, J. Gao, J. Li, Y. Zhao and Q. Zhang, Synthesis, Physical Properties, and Anion Recognition of Two Novel

Larger Azaacenes: Benzannelated Hexazaheptacene and Benzannelated N, N′-Dihydrohexazaheptacene, *Chem.–Asian J.*, 2013, **8**(7), 1574–1578.

26 P. Anzenbacher, D. S. Tyson, K. Jursíková and F. N. Castellano, Luminescence lifetime-based sensor for cyanide and related anions, *J. Am. Chem. Soc.*, 2002, **124**(22), 6232–6233.

27 O. B. Berryman, V. S. Bryantsev, D. P. Stay, D. W. Johnson and B. P. Hay, Structural criteria for the design of anion receptors: the interaction of halides with electron-deficient arenes, *J. Am. Chem. Soc.*, 2007, **129**(1), 48–58.

28 H. T. Chifotides, B. L. Schottel and K. R. Dunbar, The π-accepting arene HAT (CN) 6 as a halide receptor through charge transfer: multisite anion interactions and self-assembly in solution and the solid state, *Angew. Chem.*, 2010, **122**(40), 7360–7365.

29 P. Gamez, T. J. Mooibroek, S. J. Teat and J. Reedijk, Anion binding involving π-acidic heteroaromatic rings, *Acc. Chem. Res.*, 2007, **40**(6), 435–444.

30 B. P. Hay and V. S. Bryantsev, Anion–arene adducts: C–H hydrogen bonding, anion–π interaction, and carbon bonding motifs, *Chem. Commun.*, 2008, **21**, 2417–2428.

31 R. E. Dawson, A. Hennig, D. P. Weimann, D. Emery, V. Ravikumar, J. Montenegro, T. Takeuchi, S. Gabutti, M. Mayor and J. Mareda, Experimental evidence for the functional relevance of anion–π interactions, *Nat. Chem.*, 2010, **2**(7), 533–538.

32 J. Mareda and S. J. C. A. E. J. Matile, Anion–π slides for transmembrane transport, *Chem.–Eur. J.*, 2009, **15**(1), 28–37.

33 M. Mascal, I. Yakovlev, E. B. Nikitin and J. C. Fettinger, Fluoride-selective host based on anion–π interactions, ion pairing, and hydrogen bonding: synthesis and fluoride-ion sandwich complex, *Angew. Chem.*, 2007, **119**(46), 8938–8940.

34 B. L. Schottel, H. T. Chifotides and K. R. Dunbar, Anion-π interactions, *Chem. Soc. Rev.*, 2008, **37**(1), 68–83.

35 G. Gil-Ramírez, E. C. Escudero-Adán, J. Benet-Buchholz and P. Ballester, Quantitative evaluation of anion–π interactions in solution, *Angew Chem. Int. Ed. Engl.*, 2008, **47**(22), 4114–4118.

36 D. Miklik, S. Fatemeh Mousavi, Z. Buresova, A. Middleton, Y. Matsushita, J. Labuta, A. Ahsan, L. Buimaga-Iarinca, P. A. Karr, F. Bures, G. J. Richards, P. Svec, T. Mori, K. Ariga, Y. Wakayama, C. Morari, F. D'Souza, T. A. Jung and J. P. Hill, Pyrazinacenes exhibit on-surface oxidation-state-dependent conformational and self-assembly behaviours, *Commun. Chem.*, 2021, **4**(1), 29.

37 G. J. Richards, A. Cador, S. Yamada, A. Middleton, W. A. Webre, J. Labuta, P. A. Karr, K. Ariga, F. D'Souza, S. Kahlal, J. F. Halet and J. P. Hill, Amphiprotism-Coupled Near-Infrared Emission in Extended Pyrazinacenes Containing Seven Linearly Fused Pyrazine Units, *J. Am. Chem. Soc.*, 2019, **141**(50), 19570–19574.

38 G. J. Richards and J. P. Hill, The Pyrazinacenes, *Acc. Chem. Res.*, 2021, **54**(16), 3228–3240.

39 G. J. Richards, J. P. Hill, N. K. Subbaiyan, F. D'Souza, P. A. Karr, M. R. Elsegood, S. J. Teat, T. Mori and K. Ariga, Pyrazinacenes: aza analogues of acenes, *J. Org. Chem.*, 2009, **74**(23), 8914–8923.

40 G. J. Richards, S. Ishihara, J. Labuta, D. Miklík, T. Mori, S. Yamada, K. Ariga and J. P. Hill, Fluorescent mesomorphic pyrazinacenes, *J. Mater. Chem. C*, 2016, **4**(48), 11514–11523.

41 L. Ahrens, J. Butscher, V. Brosius, F. Rominger, J. Freudenberg, Y. Vaynzof and U. H. F. Bunz, Azaacene Dimers: Acceptor Materials with a Twist, *Chem.–Eur. J.*, 2020, **26**(2), 412–418.

42 U. Bunz, A. Appleton, S. Barlow, S. Marder and K. Hardcastle, N,N-Dihydrotetraazaheptacene: A Synthetic Strategy towards Larger Acenes with Ambient Stability, *Synlett*, 2011, **2011**(14), 1983–1986.

43 U. H. Bunz, J. U. Engelhart, B. D. Lindner and M. Schaffroth, Large N-heteroacenes: new tricks for very old dogs?, *Angew. Chem., Int. Ed.*, 2013, **52**(14), 3810–3821.

44 Z. He, R. Mao, D. Liu and Q. Miao, Highly Electron-Deficient hexaazapentacene, *Org. Lett.*, 2012, **14**(16), 4190–4193.

45 C. Z. Karaman, S. Göker, S. O. Hacioğlu, T. Hacıefendioğlu, E. Yıldırım and L. Toppare, Altering electronic and optical properties of novel benzothiadiazole comprising homopolymers via π bridges, *J. Electrochem. Soc.*, 2021, **168**(3), 036514.

46 G. P. Kini, S. K. Lee, W. S. Shin, S.-J. Moon, C. E. Song and J.-C. Lee, Achieving a solar power conversion efficiency exceeding 9% by modifying the structure of a simple, inexpensive and highly scalable polymer, *J. Mater. Chem. A*, 2016, **4**(47), 18585–18597.

47 C.-S. Ke, C.-C. Fang, J.-Y. Yan, P.-J. Tseng, J. R. Pyle, C.-P. Chen, S.-Y. Lin, J. Chen, X. Zhang and Y.-H. Chan, Molecular engineering and design of semiconducting polymer dots with narrow-band, near-infrared emission for in vivo biological imaging, *ACS Nano*, 2017, **11**(3), 3166–3177.

48 H. Reiss, F. Rominger, J. Freudenberg and U. H. Bunz, Peralkynylated Tetraazaacene Derivatives, *Chem.–Eur. J.*, 2020, **26**(5), 1013–1016.

49 S. Maier, N. Hippchen, F. Rominger, J. Freudenberg and U. H. Bunz, Cyclodimers and Cyclotrimers of 2, 3-Bisalkynylated Anthracenes, Phenazines and Diazatetracenes, *Chem.–Eur. J.*, 2021, **27**(66), 16320–16324.

50 G. Zhu and G. Zhang, Access to benzo-fused aza [7] helicene via unexpected indolization of alkyne-amine, *Org. Chem. Front.*, 2021, **8**(19), 5336–5344.

51 V. Williams and T. Swager, An improved synthesis of poly (p-phenylenebutadiynylene)s, *J. Polym. Sci., Part A: Polym. Chem.*, 2000, **38**(S1), 4669–4676.

52 J.-H. Lee, M. D. Curtis and J. W. Kampf, Unusual Thermal Polymerization of 1, 4-Bis-5-(4,4′-dialkyl-2,2′-bithiazolyl)-1, 3-butadiynes: Soluble Polymers from Diacetylenes, *Macromolecules*, 2000, **33**(6), 2136–2144.

53 J. Xu, B. Meng, J. Liu and L. Wang, A high molecular weight organometallic conjugated polymer incorporated with Hg(ii), *Chem. Commun.*, 2020, **56**(42), 5701–5704.

54 L. Xu, J. Sun, T. Tang, H. Zhang, M. Sun, J. Zhang, J. Li, B. Huang, Z. Wang and Z. Xie, Metallated graphynes as

a new class of photofunctional 2D organometallic nanosheets, *Angew Chem. Int. Ed. Engl.*, 2021, **60**(20), 11326–11334.

55 R. E. Dessy, W. L. Budde and C. Woodruff, The Formation of Carbon-Metal Bonds, *J. Am. Chem. Soc.*, 1962, **84**(7), 1172–1178.

56 R. Cross and C. Jenkins, Symmetrisation of organomercuric halides on alumina, silica and magnesium oxide, *J. Organomet. Chem.*, 1973, **56**, 125–129.

57 E. Frankland, *3.3 Product Class 3: Organometallic Complexes of Mercury*, 2004.

58 W.-Y. Wong, L. Liu and J.-X. Shi, Triplet Emission in Soluble Mercury(II) Polyyne Polymers, *Angew. Chem.*, 2003, **115**(34), 4198–4202.

59 C. L. Ho, Z. Q. Yu and W. Y. Wong, Multifunctional polymetallaynes: properties, functions and applications, *Chem. Soc. Rev.*, 2016, **45**(19), 5264–5295.

60 W.-Y. Wong and C.-L. Ho, Di-, oligo- and polymetallaynes: Syntheses, photophysics, structures and applications, *Coord. Chem. Rev.*, 2006, **250**(19–20), 2627–2690.

61 S. Saha, Anion-Induced Electron Transfer, *Acc. Chem. Res.*, 2018, **51**(9), 2225–2236.

62 T. Takeda, T. Ikemoto, S. Yamamoto, W. Matsuda, S. Seki, M. Mitsuishi and T. Akutagawa, Preparation, Electronic and Liquid Crystalline Properties of Electron-Accepting Azaacene Derivatives, *ACS Omega*, 2018, **3**(10), 13694–13703.

63 N. Jun-ichi Nishida, M. Shio, F. Eiichi, T. Hirokazu, T. Masaaki and Y. Yoshiro, Preparation, Characterization, and FET Properties of Novel Dicyanopyrazinoquinoxaline Derivatives, *Org. Lett.*, 2004, **6**(12), 2007–2010.

64 T. Du, Y. Liu, C. Wang, Y. Deng and Y. Geng, n-Type Conjugated Polymers Based on an Indandione-Terminated Quinoidal Building Block, *Macromolecules*, 2022, **55**(14), 5975–5984.

65 H. Sun, X. Guo and A. Facchetti, High-performance n-type polymer semiconductors: applications, recent development, and challenges, *Chem*, 2020, **6**(6), 1310–1326.

66 Y. Zhang, Y. Wang, C. Gao, Z. Ni, X. Zhang, W. Hu and H. Dong, Recent advances in n-type and ambipolar organic semiconductors and their multi-functional applications, *Chem. Soc. Rev.*, 2023, **52**(4), 1331–1381.

67 Y. Wang, E. Zeglio, L. Wang, S. Cong, G. Zhu, H. Liao, J. Duan, Y. Zhou, Z. Li and D. Mawad, Green Synthesis of Lactone-Based Conjugated Polymers for n-Type Organic Electrochemical Transistors, *Adv. Funct. Mater.*, 2022, **32**(16), 2111439.

68 S. R. Bheemireddy, M. P. Hautzinger, T. Li, B. Lee and K. N. Plunkett, Conjugated Ladder Polymers by a Cyclopentannulation Polymerization, *J. Am. Chem. Soc.*, 2017, **139**(16), 5801–5807.

69 H. Zhou, L. Yang, S. C. Price, K. J. Knight and W. You, Enhanced photovoltaic performance of low-bandgap polymers with deep LUMO levels, *Angew. Chem.*, 2010, **122**(43), 8164–8167.

70 J. Han, Y. Jiang, E. Tiernan, C. Ganley, Y. Song, T. Lee, A. Chiu, P. McGuiggan, N. Adams and P. J. A. C. I. E. Clancy, Blended Conjugated Host and Unconjugated Dopant Polymers Towards N-type All-Polymer Conductors and High-ZT Thermoelectrics, *Angew. Chem., Int. Ed.*, 2023, **62**(23), e202219313.

71 D. Yoo, X. Luo, T. Hasegawa, M. Ashizawa, T. Kawamoto, H. Masunaga, N. Ohta, H. Matsumoto, J. Mei and T. Mori, n-Type Organic Field-Effect Transistors Based on Bisthienoisatin Derivatives, *ACS Appl. Electron. Mater.*, 2019, **1**(5), 764–771.

72 Y. Zhou, J. Lee and L. Fang, n-Type Electron-Accepting Materials for Organic Solar Cells (OSC), in *Organic and Hybrid Solar Cells*, ed. Huang H. and Huang J., Springer International Publishing, Cham, 2014, pp. 97–119.

73 M. Ball, Y. Zhong, B. Fowler, B. Zhang, P. Li, G. Etkin, D. W. Paley, J. Decatur, A. K. Dalsania and H. Li, Macrocyclization in the design of organic n-type electronic materials, *J. Am. Chem. Soc.*, 2016, **138**(39), 12861–12867.

74 Y. Zhang, D. Hanifi, E. Lim, S. Chourou, S. Alvarez, A. Pun, A. Hexemer, B. Ma and Y. Liu, Enhancing the Performance of Solution-Processed n-Type Organic Field-Effect Transistors by Blending with Molecular "Aligners", *Adv. Mater.*, 2014, **26**(8), 1223–1228.

75 Y. Yu, C. Dong, A. F. Alahmadi, B. Meng, J. Liu, F. Jäkle and L. Wang, A p-π* conjugated triarylborane as an alcohol-processable n-type semiconductor for organic optoelectronic devices, *J. Mater. Chem. C*, 2019, **7**(24), 7427–7432.